Mody, I., Salter, M. W., & MacDonald, J. F. (1988) *Neurosci. Lett. 93*, 73–78.
Olney, J. W., & Sharpe, L. G. (1969) *Science 166*, 386–388.
Reynolds, I. J., Murphy, S. N., & Miller, R. J. (1987) *Proc. Natl. Acad. Sci. U.S.A. 84*, 7744–7748.
Simon, R. P., Swan, J. H., Griffiths, T., & Meldrum, B. S. (1984) *Science 226*, 850–852.
Snell, L. D., Morter, R. S., & Johnson, K. M. (1987) *Neurosci. Lett. 83*, 313–317.
Sorensen, R. G., & Blaustein, M. P. (1988) *Biochem. Pharmacol. 37*, 511–519.
Starmer, C. F., & Grant, A. O. (1985) *Mol. Pharmacol. 28*, 348–356.
Turski, L., Schwartz, M., Turski, W. A., Klockgether, T., Sontag, K. H., & Collins, J. F. (1985) *Neurosci. Lett. 53*, 321–326.
Vignon, J., Privat, A., Chaudrieu, I., Thierry, A., Kamenka, J. M., & Schicheportiche, R. (1986) *Brain Res. 378*, 133–141.
Watkins, J. C., & Evans, R. H. (1981) *Annu. Rev. Pharmacol. Toxicol. 21*, 165–204.
Westbrook, G. L., & Mayer, M. L. (1987) *Nature 328*, 640–643.
Woodruff, G. N., Foster, A. C., Gill, R., Kemp, J. A., Wong, E. H., & Iversen, L. L. (1987) *Neuropharmacology 26*, 903–909.

Multinuclear Magnetic Resonance Studies of the 2Fe·2S* Ferredoxin from *Anabaena* Species Strain PCC 7120. 1. Sequence-Specific Hydrogen-1 Resonance Assignments and Secondary Structure in Solution of the Oxidized Form†

Byung-Ha Oh and John L. Markley*

Department of Biochemistry, College of Agricultural and Life Sciences, University of Wisconsin—Madison, 420 Henry Mall, Madison, Wisconsin 53706

Received October 19, 1989; Revised Manuscript Received December 28, 1989

ABSTRACT: Complete sequence-specific assignments were determined for the diamagnetic ^1H resonances from *Anabaena* 7120 ferredoxin (M_r = 11 000). A novel assignment procedure was followed whose first step was the identification of the ^{13}C spin systems of the amino acids by a $^{13}C\{^{13}C\}$ double quantum correlation experiment [Oh, B.-H., Westler, M. W., Darba, P., & Markley, J. L. (1988) *Science 240*, 908–911]. Then, the ^1H spin systems of the amino acids were identified from the ^{13}C spin systems by means of direct and relayed $^1H\{^{13}C\}$ single-bond correlations [Oh, B.-H., Westler, W. M., & Markley, J. L. (1989) *J. Am. Chem. Soc. 111*, 3083–3085]. The sequential resonance assignments were based mainly on conventional interresidue $^1H^{\alpha}_i$–$^1H^N_{i+1}$ NOE connectivities. Resonances from 18 residues were not resolved in two-dimensional ^1H NMR spectra. When these residues were mapped onto the X-ray crystal structure of the homologous ferredoxin from *Spirulina platensis* [Fukuyama, K., Hase, T., Matsumoto, S., Tsukihara, T., Katsube, Y., Tanaka, N., Kakudo, M., Wada, K., & Matsubara, H. (1980) *Nature 286*, 522–524], it was found that they correspond to amino acids close to the paramagnetic 2Fe·2S* cluster. Cross peaks in two-dimensional homonuclear ^1H NMR spectra were not observed for any protons closer than about 7.8 Å to both iron atoms. Secondary structural features identified in solution include two antiparallel β-sheets, one parallel β-sheet, and one α-helix.

Plant-type ferredoxins (M_r = 11 000) belong to a class of iron–sulfur proteins that are present in virtually all organisms. Iron–sulfur proteins can be classified according to the number of iron atoms and acid-labile sulfur atoms contained in the clusters. Plant-type ferredoxins contain a 2Fe·2S* cluster ligated to the protein by four cysteine residues. Plant-type ferredoxins undergo a one-electron redox reaction with a redox potential of around −420 mV at pH 7 (Cammack et al., 1977). In the oxidized form, both iron atoms are formally Fe(III). In the reduced form, one of the iron atoms remains Fe(III) and the other becomes Fe(II). The physiological function of ferredoxin in plants and cyanobacteria is to serve as a terminal electron acceptor from photosystem I (Trebst & Avron, 1977) and subsequently to donate electrons in several reactions: reduction of $NADP^+$ to NADPH (Masaki et al., 1982), reduction of nitrite to ammonia (Ida, 1977), sulfur assimilation (Aketagawa & Tamura, 1980), and glutamate synthesis (Lea & Miflin, 1974). Plant-type ferredoxins have been sequenced from nearly 30 plants and cyanobacteria (Tsukihara et al., 1986). Crystal structures have been determined for two cyanobacterial ferredoxins (Fukuyama et al., 1980; Tsukihara et al., 1981; Tsutusi et al., 1983).

NMR[1] spectroscopy has emerged as a powerful tool for the determining solution structures of biological macromolecules. It is the only method that provides full three-dimensional structures of biomolecules such as proteins and nucleic acids in solution. NMR spectroscopy can provide, in addition, information about dynamics, kinetics, and enzyme mechanisms. The quality and content of information from NMR spectroscopy are heavily dependent on the extent of resonance assignments. Early NMR studies of 2Fe·2S* ferredoxins

†This work was supported by USDA Competitive Grant 88-37262-3406 and National Institutes of Health Grant RR02301 from the Biomedical Research Technology Program, Division of Research Resources, and made use of the National Magnetic Resonance Facility at Madison, which is supported in part by Grant RR023021. Additional equipment in the facility was purchased with funds from the University of Wisconsin, the NSF Biological Biomedical Research Technology Program (Grant DMB-8415048), the NIH Shared Instrumentation Program (Grant RR02781), and the U.S. Department of Agriculture. B.-H.O. is supported by a Peterson Fellowship from the University of Wisconsin—Madison.

*To whom correspondence should be addressed

0006-2960/90/0429-3993$02.50/0

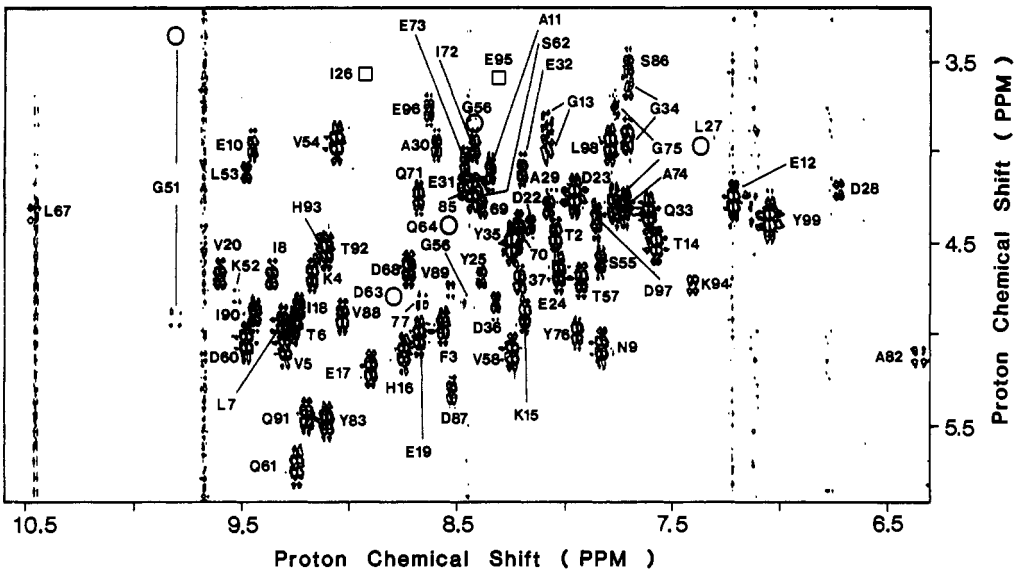

FIGURE 1: Fingerprint region ($^1H^{\alpha}$–$^1H^N$ connectivity region) of the double quantum filtered 500-MHz COSY spectrum of *Anabaena* 7120 ferredoxin. The sample was 0.5 mL of 9 mM feredoxin in 90% ^1H_2O/10% ^2H_2O containing 50 mM phosphate buffer at pH 7.1. Solvent suppression was achieved by irradiation at the solvent frequency during the relaxation delay (1.2 s). 512 blocks of FID's were collected as 2048 data points; each represented the average of 160 transients. The experiment time was 28 h. Assignments are designated by the one-letter code for amino acids followed by residue position on the amino acid sequence (Alam et al., 1986). In crowded regions, only the residue number is given. The circles indicate cross peaks visible at lower contour levels. The rectangles indicate cross peaks visible in the NOESY spectrum but not in the COSY spectrum.

mainly concerned the observation of hyperfine-shifted ^1H resonances (Poe et al., 1971; Salmeen & Palmer, 1972; Anderson et al., 1975). The ^1H and ^{13}C resonances from two histidines and four tyrosines of *Anabaena variabilis* ferredoxin I[2] were assigned on the basis of spectral comparison of several homologous proteins (Chan & Markley, 1983a,b; Chan et al., 1983).

Recently, we showed that the ^{13}C spin systems in proteins labeled uniformly with ^{13}C can be classified into 18 different amino acid types by a single $^{13}C\{^{13}C\}$ DQC experiment (Oh et al., 1988; Oh & Markley, 1989; Stockman et al., 1988a; Westler et al., 1988). The ^{13}C spin system assignments can be extended efficiently into ^1H spin system assignments by means of the $^1H\{^{13}C\}$ SBC-HH experiment as was recently demonstrated with oxidized *Anabaena* 7120 ferredoxn (Oh et al., 1989). We report here the complete sequence-specific assignments of diamagnetic ^1H resonances from oxidized *Anabaena* 7120 ferredoxin. The two following papers in this series report the complete sequence-specific assignments of diamagnetic ^{13}C and ^{15}N resonances (Oh et al., 1990) and the detection and characterization of hyperfine-shifted ^1H and ^{15}N resonances (Oh & Markley, 1990). These results represent the first extensive ^1H, ^{13}C, and ^{15}N resonance assignments of an iron–sulfur protein.

Materials and Methods

Protein Purification and Isotope Enrichment. Anabaena sp. strain PCC 7120 was grown as described by Stockman et al. (1988b). Crude ferredoxin was isolated from *Anabaena* 7120 cells by modification of the procedure of Ho et al. (1979). The dialyzed crude protein solution was loaded onto a DEAE-Sepharose fast-flow column (2.5 cm × 15 cm) equilibrated with 10 mM phosphate buffer at pH 7.5. The column was washed with the same buffer solution, and ferredoxin was eluted with 1 0 mM phosphate buffer containing 0.4 M NaCl. The ferredoxin fractions (brown color) were pooled and brought to 70% $(NH_4)_2SO_4$ saturation. The solution was allowed to stand overnight, and precipitated proteins were removed by centrifugation at 9000 rpm (Beckman JA-16 rotor) for 20 min. The resulting supernatant was brought to 100% $(NH_4)_2SO_4$ saturation and allowed to stand overnight. The brown pellet obtained by centrifuging at 9000 rpm for 20 min was dissolved in a minimal volume of 10 mM phosphate buffer at pH 7.5, containing 0.2 M NaCl, and then dialyzed against 6 L of the same buffer. The dialyzed sample was loaded onto a DEAE-52 column (3 cm × 20 cm) equilibrated with the same buffer. Ferredoxin was eluted with a linear salt gradient (0.2–0.5 M NaCl, total volume 1 L). Ferredoxin fractions with A_{420}/A_{276} ratios higher than 0.56 were considered to be pure. ^{15}N-Labeled protein, [98% U-^{15}N]ferredoxin, was produced by growing the cyanobacterium on $K^{15}NO_3$ (98+ atom %) as the sole nitrogen source.

Chemicals. The source of $K^{15}NO$ was the Mound Facility of the Monsanto Research Corp. Other chemicals were of reagent grade or better.

NMR Spectroscopy. All NMR samples consisted of 0.5 mL of 6–9 mM ferredoxin containing 50 mM phosphate buffer at pH 7.1 for samples in ^1H_2O or pH* 7.5 for samples in ^2H_2O. Samples dissolved in ^1H_2O contained 10% (v/v) ^2H_2O for the lock. Samples in ^2H_2O were prepared as follows: a 0.5-mL

[1] Abbreviations: 1D, one dimensional; 2D, two dimensional; A_{420}/A_{276}, ratio of absorbance at 420 nm to absorbance at 276 nm; COSY, correlated spectroscopy; CYCLOPS, cyclically ordered phase sequence; DQC, double quantum correlation; DQ-COSY, double quantum filtered correlated spectroscopy; FID, free induction decay; HOHAHA, homonuclear Hartmann–Hahn; NMR, nuclear magnetic resonance; NOESY, nuclear Overhauser effect spectroscopy; SBC, single-bond correlation; MBC, multiple-bond correlation; pH*, pH meter reading without correction of deuterium isotope effect; SBC-HH, single-bond correlation with Hartmann–Hahn relay; SBC-NOE, single-bond correlation with nuclear Overhauser effect; T_1, spin–lattice relaxation time; TMS, tetramethylsilane; TPPI, time proportional phase incrementation; TSP, 3-(trimethylsilyl)propionate.

[2] The protein from *Anabaena variabilis* originally was classified as a ferredoxin II on the basis of its sequence (Chan et al., 1983). According to a more recent alignment of ferredoxin sequences, it has been classified more properly as a ferredoxin I (Alam et al., 1986).

sample in ^1H_2O was lyophilized and then dissolved in 0.5 mL of ^2H_2O (99.8 atom % ^2H) to exchange labile amide protons. The sample was lyophilized once again, and the sample for NMR spectroscopy was prepared by addition of 0.5 mL of ^2H_2O (99.98 atom % ^2H). NMR data were acquired on Bruker AM-500 (11.7 T) and AM-600 (14.0 T) spectrometers. Sample temperatures were maintained at 25 °C.

DQF-COSY (Rance et al., 1983), DQ-COSY (Marion & Wüthrich, 1983), NOESY (Anil Kumar et al., 1980), HOHAHA (Davis & Bax, 1985), and $^1H\{^{15}N\}$ SBC-NOE (Shon & Opella, 1989) data were acquired in the pure absorption mode with TPPI (Marion & Wüthrich, 1983). Phase cycling for the COSY experiments was as described by Rance et al. (1983). The mixing times for NOESY experiments were 100 or 160 ms. To suppress scalar coupling effects, the mixing time was varied randomly by ±10% (Macura et al., 1982). Phase cycling for the NOESY experiments was as described by Bodenhausen et al. (1984). The mixing time for the HOHAHA experiment was 55 ms; CYCLOPS phase cycling was used to reduce quadrature images (Hoult & Richards, 1975). The HOHAHA data were collected by employing Bruker reverse electronics; the ^1H frequency was provided by the decoupler. The 90° ^1H pulse width was 30 μs. The pulse sequence used for the $^1H\{^{15}N\}$ SBC-NOE experiments was that described by Shon and Opella (1989); the NOE mixing time was 160 ms. The $^1H\{^{15}N\}$ SBC-NOE spectrum was collected by employing Bruker reverse electronics with a Bruker 5-mm inverse probe; the ^1H frequency was provided by the decoupler, and the ^{15}N frequency was provided by the transmitter with low-power amplification (90° ^{15}N pulse width = 190 μs). WALTZ-16 ^{15}N decoupling (Shaka et al., 1983) was used during acquisition to collapse ^1H–^{15}N splittings.

^1H chemical shifts are referenced to internal TSP. ^{15}N chemical shifts are referenced to liquid ammonia; the resonance of external [^{15}N]ammonium sulfate used as the external standard was assumed to be 21.6 ppm at 25 °C. The ^{13}C chemical shifts are referenced to external tetramethylsilane; the dioxane signal, which was an external standard, was taken to be 67.8 ppm at 25 °C.

Results

The fingerprint region of the COSY spectrum of *Anabaena* 7120 ferredoxin is shown in Figure 1. The sequence-specific assignments shown were arrived at in three stages. In the first stage, amino acid ^{13}C spin systems were traced and classified by the $^{13}C\{^{13}C\}$ DQC (Oh et al., 1988) and $^{13}C\{^{15}N\}$ SBC (Mooberry et al., 1989) experiments. In the second stage, the ^{13}C spin system identifications were extended to $^1H^{\alpha}$,$^1H^N$ cross peaks in the fingerprint region of the COSY spectrum mostly by the $^1H\{^{13}C\}$ SBC-HH*H* experiment (Oh et al., 1989). On the basis of better $^1H\{^{13}C\}$ SBC-HH data obtained with a longer Hartmann–Hahn mixing time (data not shown), we made four more identifications that later were shown to correspond to His[16], Glu[17], Ile[26], and Tyr[76]. At this stage, we had classified 60 of the 79 observed COSY fingerprint peaks according to 15 different amino acid types. The classification was limited to 15 of the 20 possible normal amino acid types for the following reasons: (1) Trp and Met are absent in *Anabaena* 7120 ferredoxin. (2) Paramagnetic broadening of the single Arg and all four Cys residues in the protein prevented their observation in the COSY spectrum (see below). (3) The $^{13}C^{\beta}$ of the single diamagnetic Phe (Phe[3]) was not resolved from other ^{13}C spin systems. The third stage involved the assignment of the cross peaks to specific amino acid residues in the protein. A search was conducted for $^1H^{\alpha}$–$^1H^N$ ($d_{\alpha N}$), $^1H^{\beta}$–$^1H^N$ ($d_{\beta N}$), and $^1H^N$–$^1H^N$ (d_{NN}) sequential NOE

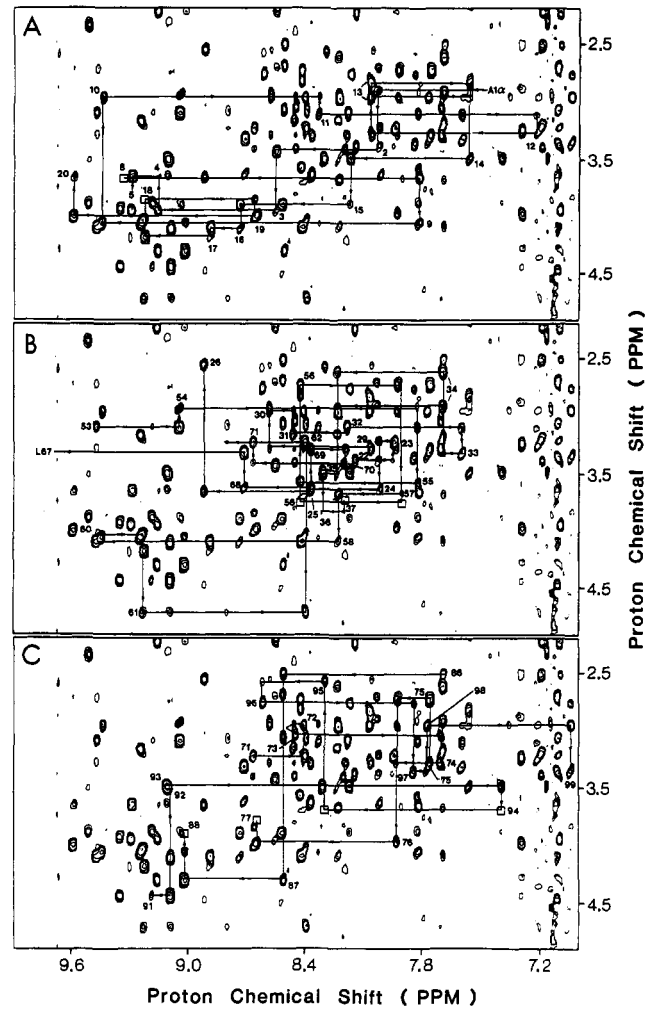

FIGURE 2: Fingerprint region of the 500-MHz NOESY spectrum of *Anabaena* 7120 ferredoxin. The sample was the same as described in Figure 1. 512 blocks of FID's were collected as 2048 data points; each represented the average of 160 transients. The NOE mixing time was 100 ms. Assignments are designated by residue numbers only. The fingerprint region is shown three times with different sequential connectivities indicated: (A) 1–5 and 8–20; (B) 22–26, 29–37, 53–63, and 67–71; (C) 71–77, 86–88, and 91–99.

connectivities (Wüthrich, 1986) between neighboring amino acids. Connectivities thus obtained were compared with the known amino acid sequence of the protein (Alam et al., 1986). This procedure was facilitated by the extensive spin-system assignments and classifications by amino acid type made in the second stage.

Sequential NOE Connectivities. The assignment of the $^1H^{\alpha}$,$^1H^{\beta}$ COSY cross peak from Ala[1] was based on the strong $^{15}N^{\alpha}$,$^1H^{\beta}$ cross peak observed in the $^1H\{^{15}N\}$ MBC spectrum (Oh et al., 1990; Figure 6). Because of the rapid exchange of the amino-terminal protons of Ala[1] with ^1H_2O, this residue does not provide a COSY $^1H^{\alpha}$,$^1H^N$ cross peak. The assignment of Thr[2] was based on an interresidue NOE cross peak between its $^1H^N$ and the $^1H^{\alpha}$ of Ala[1] (Figure 2A). This run of $^1H^{\alpha}_i$–$^1H^N_{i+1}$ NOE cross peaks was continued sequentially to Val[20] (Figures 2A and 4) and served to identify the cross peaks from Phe[3] and Glu[12] in the COSY fingerprint region. All other cross peaks in this segment had been identified previously by amino acid type, and the sequential connectivities converted them into sequence-specific assignments. The $^1H^{\delta}$'s of proline residues can be identified easily because of the characteristic position of $^{13}C^{\delta}$,($^1H^{\delta}$,$^1H^{\delta'}$) cross peaks on the $^1H\{^{13}C\}$ SBC map (Oh et al., 1990; Figure 1). One of the three identified Pro$^1H^{\delta}$

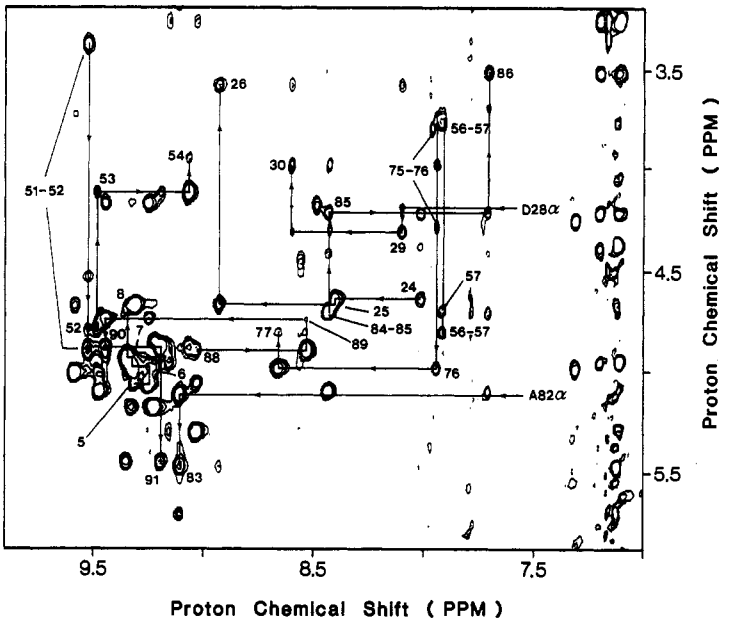

FIGURE 3: Fingerprint region of the 600-MHz NOESY spectrum of *Anabaena* 7120 ferredoxin. The sample consisted of 0.5 mL of 9 mM ferredoxin dissolved in ^2H_2O containing 50 mM phosphate buffer at pH* 7.5. 512 blocks of FID's were collected as 4096 data points; each represented the average of 104 transients. The NOE mixing time was 160 ms. The residual water peak was not irradiated. Assignments are designated by residue numbers only. In the labeling scheme used, A–B represents a NOE cross peak where A and B stand for residue i and $i + 1$, respectively. The sequential connectivities shown in this figure are mainly the ones obscured by water irradiation in Figure 2: 5–8, 24–26, 28–30, 51–54, 56–57, 75–77, 82–86, and 88–91.

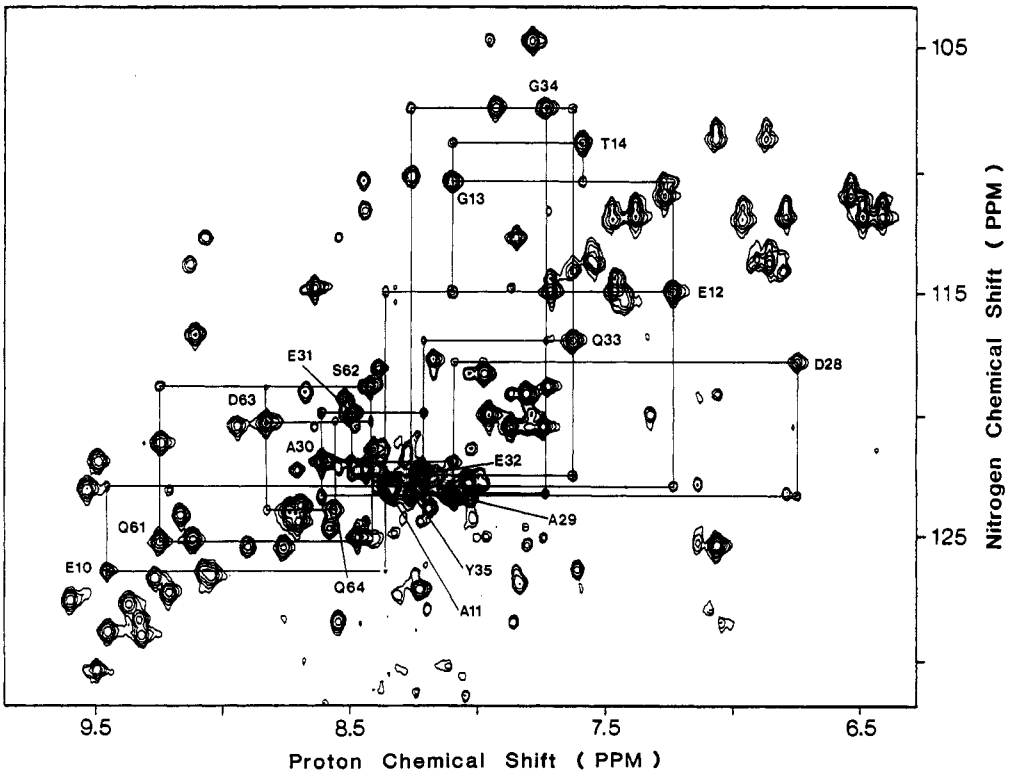

FIGURE 4: Selected region of the 600-MHz $^1H\{^{15}N\}$ SBC-NOE spectrum of oxidized [95% U-^{15}N]ferredoxin from *Anabaena* 7120. The sample consisted of 0.5 mL of 6.0 mM ferredoxin in 90% ^1H_2O/10% ^2H_2O containing 50 mM phosphate buffer at pH 7.1. 512 blocks of FID's were collected as 4096 data points; each represented the average of 88 transients. Solvent suppression was achieved by irradiation at the solvent frequency during the relaxation delay (1.0 s) and NOE mixing time (160 ms). The sequential d_{NN} connectivities are shown for residues 10–14, 28–35, and 61–64. This spectrum also contains sequential d_{NN} connectivities for residues 69–76 and 94–99. The assignments of ^1H–^{15}N single-bond correlation cross peaks are described in the second paper in this series (Oh et al., 1990). The absence of diagonal peaks in this experiment allowed the detection of NOE cross peaks between correlated $^1H^N$ resonances having similar chemical shifts whose NOE connectivities were not observed in the ^1H NOESY spectrum because of interference from the negative tail of the diagonal.

pairs shows NOE cross peaks to Val^{20} $^1H^\alpha$ (data not shown). This assigns these signals to the unique dipeptide Val^{20}-Pro^{21}. The Pro^{21} $^1H^\alpha$ peak is very close to the water peak so that the Pro^{21} $^1H^\alpha$ to Asp^{22} $^1H^N$ NOE cross peak was bleached. Thus, the assignment of the next residue, Asp^{22}, was postponed temporarily.

The next peptide segment identified was residues 28–37. The unique tripeptide sequence of Asp^{28}-Ala^{29}-Ala^{30} shows

clear $^1H^{\alpha}$–$^1H^N$ connectivities in the NOESY spectrum recorded in ^2H_2O (Figure 3). This sequence was extended to Ala[30]-E-E-X-G-Y-X-L by $^1H^{\alpha}_i$–$^1H^N_{i+1}$ NOE connectivities (Figure 2B). X indicates a cross peak whose first-order assignment was not determined previously. The sequential assignments identified the fingerprint region cross peaks of Gln[33] and Asp[36]. Two Pro[38] $^1H^{\delta}$'s showed $d_{\alpha\delta}$ NOE connectivities to Leu[37] (data not shown). The assignments up to residue 38 included all but the six-residue stretch, 22–27.

Resonance from the peptide segment[3] 51–64 were assigned by sequential $d_{\alpha N}$ or d_{NN} connectivities that provided the sequence G-K-L-V-S-G-T-V-X-Q-X-X-X, which identified the fingerprint region cross peaks of Asp[60], Ser[62], and Gln[64] (Figures 2B and 4). The chemical shift of the Asp[63] $^1H^{\alpha}$ is very close to the water peak, and the Asp[63]-Gln[64] $d_{\alpha N}$ NOE cross peak was not observed as a consequence of water peak irradiation. We assigned the $^1H^N$ of Gln[64] on the basis of sequential d_{NN} connectivities for Ser[62]-Asp-[63]-Gln[64] detected in the $^1H\{^{15}N\}$ SBC-NOE spectrum (Figure 4).

The peptide segment 67–77 was identified by sequential $d_{\alpha N}$ connectivities of X-X-X-D-Q-I-E-A-G-Y-V (Figure 2B,C). In this segment, Leu[67], Asp[68], and Asp[69] were located by sequential assignments.

Assignment of peptide segment 82–99 was based on the sequential NOE connectivities of A-Y-P-T-S-D-V-V-I-Q-T-H-K-X-E-X-L-X. These sequential assignments identified the resonances of Glu[95], Asp[97], and Tyr[99]. Strong $d_{\alpha\delta}$ cross peaks between Tyr[83] $^1H^{\alpha}$ and Pro[84] $^1H^{\delta}$,$^1H^{\delta'}$ were identified in the NOESY spectrum (data not shown). Pro[84] $^1H^{\alpha}$ shows a NOE cross peak to Thr[85] $^1H^N$ (Figure 3). The $d_{\alpha N}$ NOE cross peak of Lys[94]-Glu[95] was bleached by water saturation. The Glu[95] assignment resulted from observed $d_{\beta N}$ (data not shown) and d_{NN} (Figure 4) connectivities between Lys[94] and Glu[95]. With the exception of this dipeptide, we observed all expected sequential $d_{\alpha N}$ connectivities for this 18-residue peptide segment (Figures 2C and 3).

The peptide segment 22–26 was identified by sequential $d_{\alpha N}$ connectivities of X-X-E-X-I, which located resonances of Asp[22], Asp[23], and Tyr[25]. It was easily assigned because only a few cross peaks in the NOESY fingerprint region remained unassigned at this stage. The next residue, Leu[27], shows only a $^1H^{\alpha}$,$^1H^N$ cross peak in the COSY (Figure 1) and NOESY spectra but no NOE cross peaks to adjacent residues except for a $^1H^{\beta}$,$^1H^N$ NOE cross peak to Ile[26] (data not shown). The assignment of the Leu[27] COSY fingerprint cross peak was confirmed by the observation of a sequential $^{13}C'$,$^{15}N^{\alpha}$ cross peak from Ile[26]-Leu[27] in the $^{13}C\{^{15}N\}$ SBC spectrum (Oh et al., 1990; Figure 3).

The region 0.05 ppm to either side of water peak was bleached when the water peak was irradiated. In cases where this obscured NOE peaks located close to the water peak, the NOESY spectrum recorded in ^2H_2O (Figure 3) was used to follow some of the connectivities. Figure 3 shows such sequential $d_{\alpha N}$ connectivities. In other cases, the NOESY spectrum (^2H_2O) removed ambiguities in sequential assignments arising from overlapping $^1H^N$ or $^1H^{\alpha}$ chemical shifts in the NOESY (^1H_2O) spectrum. When overlaps obscured sequential connectivities in the fingerprint region, identification of both $^1H^{\alpha}_i$–$^1H^N_{i+1}$ and $^1H^{\beta}_i$–$^1H^N_{i+1}$ cross peaks (Englander & Wand, 1987) led to consistent sequential connectivities.

Assignments of Side-Chain Spin Systems. A total of 41 peptide backbone $^1H^N$ resonances were linked to side-chain spin systems by HOHAHA (Figure 5) and RELAY data (Oh et al., 1989) recorded in ^1H_2O or ^2H_2O. The remaining $^1H^N$ resonances were linked to side chains by COSY and NOESY data. Overlaps in the aliphatic region of the COSY spectrum frequently interfered with the tracing of scalar coupling connectivities. This problem was overcome by use of RELAY or HOHAHA data sets (not shown), and virtually all observed cross peaks in this region were assigned specifically.

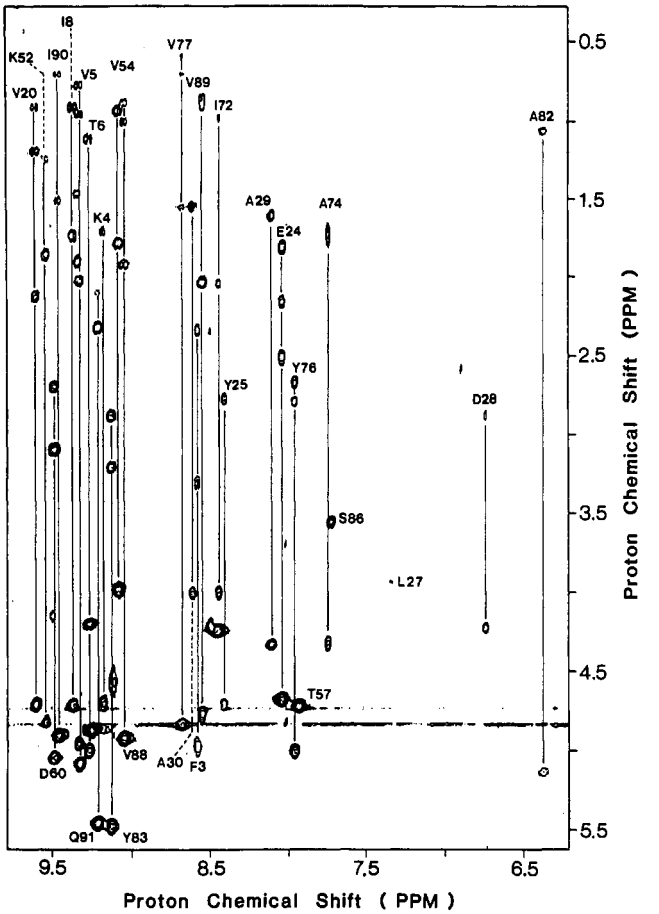

FIGURE 5: 600-MHz HOHAHA spectrum of *Anabaena* 7120 ferredoxin. The sample was the same as described in Figure 3. 512 blocks of FID's were collected as 4096 data points; each represented the average of 104 transients. HOHAHA connectivities are drawn for slowly exchanging amide protons. Assignments are given by amino acid type and residue number.

The $^1H^{\alpha}$,$^1H^{\beta}$ COSY cross-peak assignments are presented in Figure 6. In this region of the spectrum, four cross peaks (labeled with "?") were not assigned. The $^1H^{\alpha}$,$^1H^N$ COSY and NOE cross peaks of Ser[65] were not observed. However, its $^1H^{\alpha}$,($^1H^{\beta}$,$^1H^{\beta'}$) cross peaks were assigned on the basis of the corresponding C^{β},($^1H^{\beta}$,$^1H^{\beta'}$) cross peaks identified in the $^1H\{^{13}C\}$ SBC spectrum (Oh et al., 1990; Figure 1). The $^1H^{\alpha}$ chemical shift of Ser[65] coincides with the water peak. The $^1H^{\alpha}$,$^1H^N$ COSY or NOE cross peaks of Ser[65] were not observed. The expected cross peak appears to be obscured by water-peak irradiation rather than by paramagnetic broadening, since the H^N of this residue is too far from the iron atoms in the crystal structure to be broadened (Table II).

Aromatic resonances usually are connected to their aliphatic resonances by intraresidue NOE cross peaks between $^1H^{\beta}$ and $^1H^{\delta}$. We assigned the observed aromatic resonances from *Anabaena* 7120 ferredoxin by this approach except for those from Tyr[83] and Tyr[99], whose cross peaks were not resolved in the NOESY spectrum (data not shown). We were able to assign these resonances, however, by using scalar coupling

[3] The *Anabaena* 7120 sequence does not have a residue 59 because of a deletion at this position in the numbering system used (Hase et al., 1978).

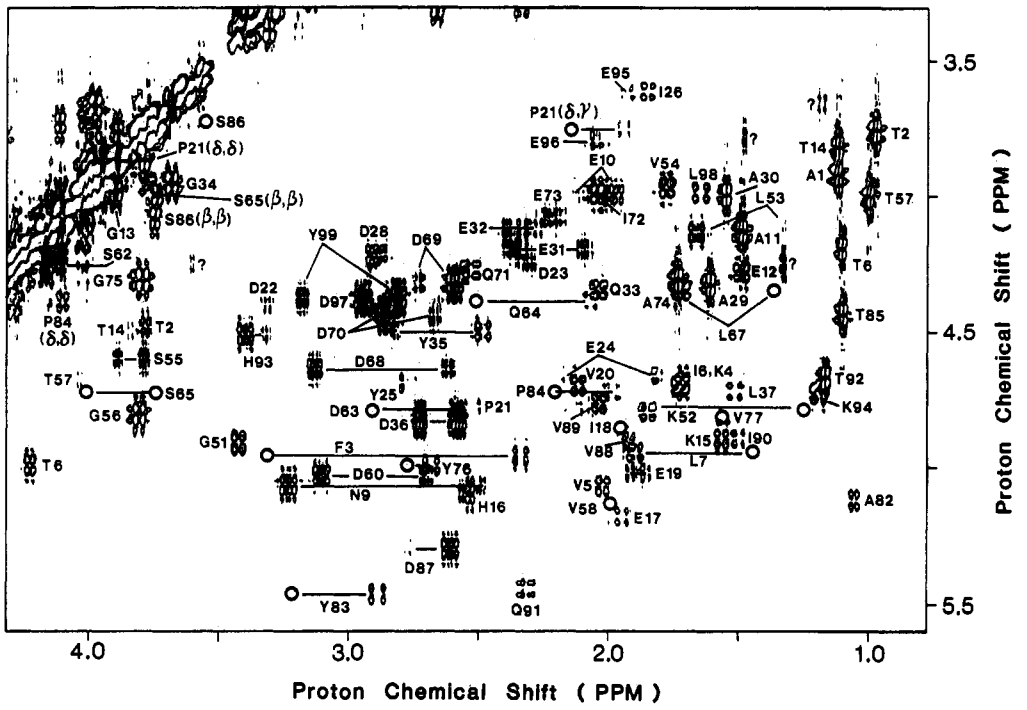

FIGURE 6: Aliphatic region of the 600-MHz COSY spectrum of *Anabaena* 7120 ferredoxin. The sample was the same as described in Figure 3. 512 blocks of FID's were collected as 4096 data points; each represented the average of 112 transients. The cross peaks represent $^1H^{\alpha}$–$^1H^{\beta}$ scalar coupling connectivities unless indicated otherwise. Assignments are designated by residue numbers only.

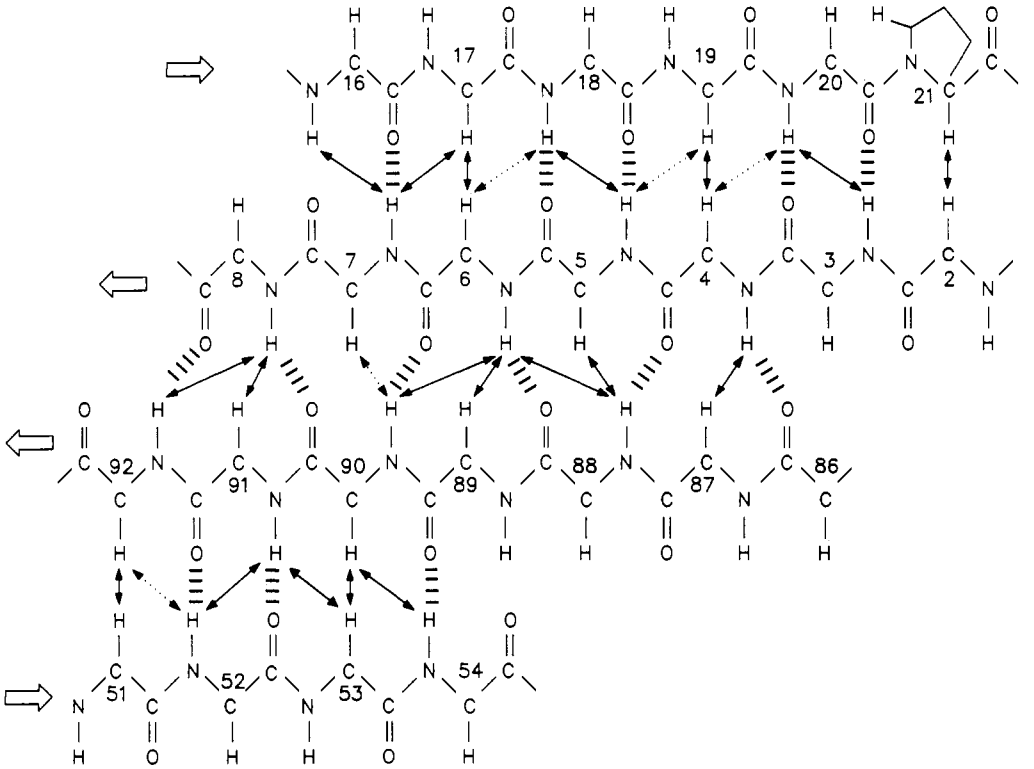

FIGURE 7: Secondary β-sheet structure identified by interresidue NOE's (solid arrows). Dotted arrows indicate expected, but unobserved, NOE cross peaks that probably were obscured by irradiation of the water peaks. Broken lines represent hydrogen bonds as indicated by amide protons that survive ≤30-h exchange in ^2H_2O (during sample preparation and NMR data acquisition).

pathways (Stockman et al., 1989). The $^1H^{\alpha}$ assignments of Tyr^{83} and Tyr^{99} were extended to $^{13}C^{\alpha}$ by means of $^1H\{^{13}C\}$ SBC data. The $^{13}C^{\alpha}$ assignments were then extended to aromatic carbon assignments by following ^{13}C-^{13}C connectivities in the $^{13}C\{^{13}C\}$ DQC data. Then the aromatic protons were cross assigned in the $^1H\{^{13}C\}$ SBC spectrum (Oh et al., 1990; Figure 8).

The carboxamide protons of all Asn (1) and Gln (5) residues were identified on the basis of their pairs of ^1H–^{15}N single-bond correlation peaks in the $^1H\{^{15}N\}$ SBC spectrum (Oh et al., 1990; Figure 4). Their sequence-specific assignments derived from assignments of the carboxamide nitrogens (Oh et al., 1990). The Asn^9 $^{15}N^{\delta}$ and Gln^{91} $^{15}N^{\epsilon}$ resonances overlap in the $^1H\{^{15}N\}$ SBC spectrum. These were assigned individually

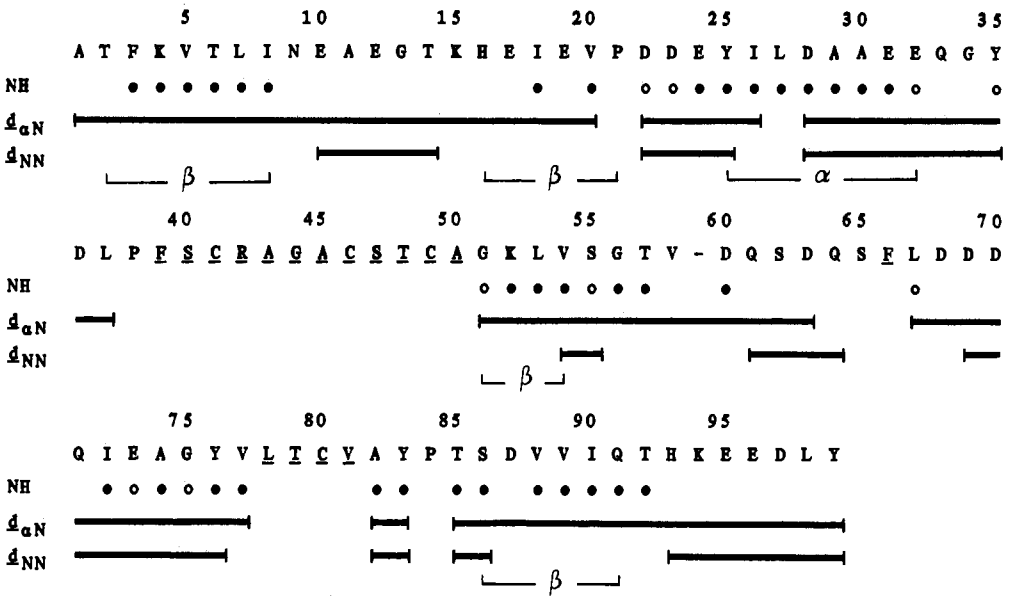

FIGURE 8: Amino acid sequence of the *Anabaena* 7120 ferredoxin with NOE connectivities used in the sequential assignment procedure and hydrogen-exchange data. The black circles above the sequence indicate slowly exchanging amide protons as defined by the observation of a cross peak in the fingerprint region of the HOHAHA and NOESY maps taken 30 h after sample preparation in ^2H_2O. Open circles above the sequence indicate amide protons that survived after 8 h in ^2H_2O as defined by the observation of cross peaks in the $^1H\{^{15}N\}$ SBC spectrum taken in ^2H_2O (Oh et al., 1990; Figure 5). Amino acids whose $^1H^\alpha$,$^1H^N$ cross peaks were not observed in both the COSY and NOESY spectra because of paramagnetic perturbation are underlined. Secondary structural elements determined from the NMR data are indicated. Residues 69–77 show strong d_{NN} connectivities characteristic of α-helix. However, the amide proton exchange rates of residues 72–77 are not uniformly slow. If this is helical, it would be less rigid than the α-helical segment containing residues 25–33. For comparison, the amino acid sequence of *Spirulina platensis* ferredoxin is provided: ATYKVTLINEAEGINETIDCDDDTYILDAAEEAGLDLPYSCRAGACSTCAGTITS-GTI-DQSDQSFLDDDQIEAGYVLTCVAYPTSDCTIKTHQEEGLY.

by identifying $^1H^\delta$,$^1H^\beta$ and $^1H^\epsilon$,$^1H^\gamma$ intraresidue cross peaks from Asn^9 and Gln^{91}, respectively, in the NOESY spectrum (data not shown).

Discussion

Structure. Interresidue NOE cross peaks were identified and used to elucidate the secondary structure of *Anabaena* 7120 ferredoxin in solution. We were able to construct two antiparallel β-sheets and one parallel β-sheet (Figure 7). The hydrogen-bonding patterns between the polypeptide strands were confirmed by the slow exchange rates of the amide protons (Figure 5) expected to make hydrogen bonds in the β-sheets. Residues 2–8 serve as a central strand for one antiparallel β-sheet with residues 16–21 and for one parallel β-sheet with residues 86–92. Residues 9–15 constitute a β-turn, which connects the antiparallel β-sheet. Strong d_{NN} connectivities were observed for the sequence 10–14 (Figure 4).

Residues 51–54 adopt an antiparallel β-sheet conformation with part of the 86–92 β-strand. We also identified one α-helix (which includes residues 25–32) on the basis of strong d_{NN} NOE cross peaks observed in the $^1H\{^{15}N\}$ SBC-NOE spectrum (Figure 4) and small $^3J_{\alpha N}$ coupling constants as manifested by weak $^1H^\alpha$,$^1H^N$ cross peaks in the COSY spectrum in ^2H_2O (Oh et al., 1990; Figure 5). Slow exchange rates were observed for the amide protons of residues 25–32 in the α-helix. The interresidue NOE patterns and qualitative amide exchange data are summarized in Figure 8. In the identified α-helix, the signals from Leu^{27} were weak owing to paramagnetic broadening of its amide proton. Even though it is in the core of the helix, d_{NN} connectivities to Ile^{26} and Asp^{28} were not detected.

The identified secondary structure (Figures 7 and 8) is very similar to that found in the X-ray structures of the homologous ferredoxins from *Spirulina platensis* (Tsukihara, 1981) and *Aphanothece sacrum* (Tsutusi et al., 1983). In addition to showing that the gross conformation does not change on crystallization, this indicates that the overall backbone conformations of related ferredoxins having 72–81% amino acid sequence homology are strongly conserved.

Paramagnetic Effects. ^1H resonance assignments are summarized in Table I along with the ^{13}C and ^{15}N assignments (Oh et al., 1990). *Anabaena* 7120 ferredoxin contains several amino acids whose observed spin systems were incomplete (missing cross peaks in ^1H 2D NMR spectra). This suggests that these residues are located on the "border line" between the parmaganetic and diamagnetic parts of the protein such that resonances from a fraction of each residue are observed in 2D NMR spectra. Some of these resonances could be assigned to particular residues in the sequence through NOE connectivities to adjacent amino acids or by other information. One example is Leu^{27}, which shows a $^1H^\alpha$,$^1H^N$ cross peak but lacks the rest of the expected COSY connectivities. The resonances from side-chain nuclei must be broadened by the 2Fe·2S* center in accordance with the observation that the side chain of this residue is pointing toward the 2Fe·2S* center in the X-ray crystal structure of homologous ferredoxin (Tsukihara et al., 1981). Such amino acids are indicated by an asterisk (*) in Table I. On the other hand, four observed peaks in the aliphatic region of the COSY spectrum were not assigned owing to the lack of any sequential connectivities to adjacent amino acids; they are labeled "?" in Figure 6.

After assignment of all resolved $^1H^\alpha$,$^1H^N$ cross peaks in the COSY fingerprint region, 18 amino acids remained unaccounted for: Phe^{39}-Ser^{40}-Cys^{41}-Arg^{42}-Ala^{43}-Gly^{44}-Ala^{45}-Cys^{46}-Ser^{47}-Thr^{48}-Cys^{49}-Ala^{50}, Ser^{65}-Phe^{66}, and Leu^{78}-Thr^{79}-Cys^{80}-Val^{81}. In the crystal structure of the homologous ferredoxin from *Spirulina platensis*, the H^α and H^N atoms of all these residues, except Ser^{65}, are located close to the 2Fe·2S* center (Figure 9 and Table II). The peptide segment Cys^{41}-Arg^{42}-Ala^{43}-Gly^{44}-Ala^{45}-Cys^{46}-Ser^{47}-Thr^{48}-Cys^{49} forms

Table I: Chemical Shifts (ppm) of the Assigned ^{1}H, ^{13}C, and ^{15}N NMR Resonances of Oxidized *Anabaena* 7120 Ferredoxin in 50 mM Phosphate Buffer at pH 7.1[a]

residue		H^N [N]	α	β	γ	δ	others
Ala-1	^{1}H [^{15}N]	[40.8]	3.92	1.13			
	^{13}C		50.0	18.1			C′ = 171.3
Thr-2	^{1}H [^{15}N]	8.06 [114.5]	4.49	3.74	0.99		
	^{13}C		59.2	69.1	22.3		C′ = 170.8
Phe-3	^{1}H [^{15}N]	8.58 [124.7]	4.98	3.30, 2.34		7.13	H^{ϵ} = 7.21; H^{ζ} = 7.11
	^{13}C		55.3	41.2	136.3	130.0	C^{ϵ} = 129.2; C^{ζ} = 128.0
Lys-4	^{1}H [^{15}N]	9.17 [124.1]	4.70	1.73, 1.28	1.48, 1.41	1.69, 1.76	H^{ϵ} = 3.08, 2.92; N^{ζ} = 33.1
	^{13}C		54.3	31.2	23.1	27.3	C^{ϵ} = 40.1; C′ = 174.7
Val-5	^{1}H [^{15}N]	9.33 [129.1]	5.09	2.03	0.96, 0.78		
	^{13}C		59.1	32.3	20.0, 19.2		
Thr-6	^{1}H [^{15}N]	9.27 [126.7]	5.01	4.21	1.12		
	^{13}C		60.4	67.6	19.6		C′ = 171.5
Leu-7	^{1}H [^{15}N]	9.35 [128.4]	4.96	1.91, 1.48	1.65	0.73, 0.62	
	^{13}C		51.5	41.0	24.6	24.5, 21.4	
Ile-8	^{1}H [^{15}N]	9.37 [127.7]	4.70	1.74	1.46, 0.91	0.77	$(CH_3)^{\gamma}$ = 0.91
	^{13}C		58.7	39.5	26.0	12.0	$(CH_3)^{\gamma}$ = 15.1
Asn-9	^{1}H [^{15}N]	7.84 [126.7]	5.08	3.22, 2.48			H^{δ} = 6.80, 6.42; N^{δ} = 111.8
	^{13}C		49.5	36.3	175.0		C′ = 174.9
Glu-10	^{1}H [^{15}N]	9.45 [126.3]	4.00	2.11, 1.99	2.31, 2.20		
	^{13}C		57.7	29.2	35.6	182.0	
Ala-11	^{1}H [^{15}N]	8.35 [122.8]	4.13	1.50			
	^{13}C		53.3	16.7			C′ = 178.2
Glu-12	^{1}H [^{15}N]	7.23 [115.0]	4.29	2.18, 1.51	2.23		
	^{13}C		54.2	29.6	35.2		C′ = 175.5
Gly-13	^{1}H [^{15}N]	8.09 [110.4]	(4.01, 3.89)				
	^{13}C		44.8				C′ = 173.6
Thr-14	^{1}H [^{15}N]	7.58 [108.9]	4.50	3.83	1.13		
	^{13}C		57.9	70.2	19.9		
Lys-15	^{1}H [^{15}N]	8.20 [123.7]	4.91	1.57	1.17, 1.10	1.58	H^{ϵ} = 2.84; N^{ζ} = 33.7
	^{13}C		54.0	33.1	23.3	27.7	C^{ϵ} = 39.9
His-16	^{1}H [^{15}N]	8.75 [125.3]	5.12	2.57, 2.55		$H^{\delta 2}$ = 6.89	$H^{\epsilon 1}$ = 7.99; $N^{\delta 1}$ = 213.8; $N^{\epsilon 2}$ = 183.8
	^{13}C		52.5	31.9	132.6	$C^{\delta 2}$ = 119.2	$C^{\epsilon 1}$ = 136.1
Glu-17	^{1}H [^{15}N]	8.91 [125.3]	5.21	1.94	2.16		
	^{13}C		53.8	30.3	35.2		
Ile-18	^{1}H [^{15}N]	9.25 [121.1]	4.88	1.95	1.40, 1.11	0.67	$(CH_3)^{\gamma}$ = 1.98
	^{13}C		57.8	40.7	24.1	12.7	$(CH_3)^{\gamma}$ = 17.5
Glu-19	^{1}H [^{15}N]	8.68 [123.6]	5.04	1.90, 1.82	2.23, 2.02		
	^{13}C		53.7	29.6	35.2		
Val-20	^{1}H [^{15}N]	9.60 [127.4]	4.71	2.12	1.19, 0.92		
	^{13}C		57.8	34.0	20.3, 21.7		C′ = 171.7
Pro-21	^{1}H [^{15}N]	[139.3]	4.79	2.91	2.20, 1.95	3.97, 3.77	
	^{13}C		61.2	31.9	26.5	50.3	C′ = 174.3
Asp-22	^{1}H [^{15}N]	8.67 [117.7]	4.40	3.31, 2.66			
	^{13}C		57.1	37.9			
Asp-23	^{1}H [^{15}N]	7.96 [118.2]	4.25	2.90, 2.31			
	^{13}C		50.5	37.9			
Glu-24	^{1}H [^{15}N]	8.04 [122.8]	4.67	2.17, 1.81	2.51		
	^{13}C		53.0	31.4	33.7	181.0	
Tyr-25	^{1}H [^{15}N]	8.42 [121.3]	4.70	2.78		6.39	
	^{13}C		53.0	37.0	128.0	130.4	C^{ϵ} = 116.0; C^{ζ} = 154.8; C′ = 177.7
Ile-26	^{1}H [^{15}N]	8.95 [120.6]	3.61	1.86	2.28, 1.04	0.76	$(CH_3)^{\gamma}$ = 0.78
	^{13}C		65.3	37.3	29.3	12.0	$(CH_3)^{\gamma}$ = 14.6; C′ = 175.3
*Leu-27	^{1}H [^{15}N]	7.33 [116.7]	3.94				
	^{13}C		57.9	41.2			
Asp-28	^{1}H [^{15}N]	6.75 [117.9]	4.23	2.87			
	^{13}C		55.9	38.8			
Ala-29	^{1}H [^{15}N]	8.12 [123.4]	4.33	1.62			
	^{13}C		53.4	19.1			C′ = 178.2
Ala-30	^{1}H [^{15}N]	8.61 [121.9]	3.99	1.57			
	^{13}C		54.4	16.5			
Glu-31	^{1}H [^{15}N]	8.48 [120.0]	4.20	2.38, 2.10	2.57		
	^{13}C		57.8	28.7	35.1		
Glu-32	^{1}H [^{15}N]	8.35 [122.4]	4.12	2.38, 2.30	2.52, 2.43		
	^{13}C		57.6	27.9	34.9		C′ = 176.9
Gln-33	^{1}H [^{15}N]	7.62 [116.9]	4.35	2.73, 2.05	2.69, 2.58		H^{ϵ} = 7.73, 7.48; N^{ϵ} = 114.8
	^{13}C		54.4	27.8	32.2	178.9	C′ = 173.4
Gly-34	^{1}H [^{15}N]	7.73 [107.4]	(3.96, 3.68)				
	^{13}C		43.8				C′ = 172.4
Tyr-35	^{1}H [^{15}N]	8.27 [123.1]	4.50	2.81, 2.49		6.80	H^{ϵ} = 6.34
	^{13}C		56.0	36.9	129.3	130.7	C^{ϵ} = 116.1; C^{ζ} = 154.8
Asp-36	^{1}H [^{15}N]	8.34 [123.0]	4.84	2.73, 2.58			
	^{13}C		52.4	40.0	178.9		
Leu-37	^{1}H [^{15}N]	8.22 [127.0]	4.73	2.01, 1.53	1.67	1.07, 0.86	
	^{13}C		50.4	41.6	26.0	22.0, 23.9	C′ = 173.2
Pro-38	^{1}H [^{15}N]	[134.3]	4.40			3.20, 3.15	
	^{13}C		61.2	30.7	26.3	48.0	C′ = 175.0

Table I (Continued)

residue		H^N [N]	α	β	γ	δ	others
*Phe-39	^{1}H [^{15}N]						H^ϵ = 7.23; H^ζ = 7.34
	^{13}C				136.3	132.2	C^ϵ = 130.4; C^ζ = 129.9
Ser-40							
Cys-41							
*Arg-42	^{1}H [^{15}N]						H^ϵ = 7.13; N^ϵ = 84.9; N^η = 73.2, 71.4
	^{13}C						C^ζ = 157.1
Ala-43							
Gly-44							
Ala-45							
Cys-46							
Ser-47							
Thr-48							
Cys-49							
*Ala-50	^{1}H [^{15}N]			1.20			
	^{13}C		52.0	17.7			C′ = 176.9
Gly-51	^{1}H [^{15}N]	9.82 [113.1]	(4.93, 3.41)				
	^{13}C		42.3				C′ = 169.6
Lys-52	^{1}H [^{15}N]	9.54 [123.1]	4.81	1.86, 1.24	1.07, 0.29	1.43	H^ϵ = 2.73, 1.31; N^ζ = 35.0
	^{13}C		53.6	36.1	23.9	27.9	C^ϵ = 40.5; C′ = 173.6
Leu-53	^{1}H [^{15}N]	9.50 [130.3]	4.14	1.67, 1.29	1.50	0.81, 0.67	
	^{13}C		55.0	41.2	25.4	21.6, 22.7	C′ = 175.3
Val-54	^{1}H [^{15}N]	9.09 [126.4]	3.97	1.79	0.93, 0.93		
	^{13}C		62.2	31.4	20.0, 18.8		C′ = 174.7
Ser-55	^{1}H [^{15}N]	7.84 [112.7]	4.62	3.88, 3.78			
	^{13}C		56.3	63.2			
Gly-56	^{1}H [^{15}N]	8.44 [110.5]	(4.83, 3.79)				
	^{13}C		42.3				C′ = 170.7
Thr-57	^{1}H [^{15}N]	7.94 [107.4]	4.73	4.02	1.01		
	^{13}C		57.9	70.7	19.7		C′ = 171.7
Val-58	^{1}H [^{15}N]	8.27 [110.2]	5.12	2.01	0.76, 0.73		
	^{13}C		56.5	34.5	20.5, 17.0		C′ = 173.4
Asp-60	^{1}H [^{15}N]	9.49 [121.9]	5.05	3.10, 2.49			
	^{13}C		51.6	41.1	179.1		
Gln-61	^{1}H [^{15}N]	9.26 [125.1]	5.74	1.39	2.48, 2.29		H^ϵ = 7.06, 6.86; N^ϵ = 108.6
	^{13}C		51.1	26.4	30.1	176.0	
Ser-62	^{1}H[^{15}N]	8.43 [118.8]	4.27	4.15, 4.08			
	^{13}C		60.9	61.7			C′ = 173.7
Asp-63	^{1}H [^{15}N]	8.83 [120.3]	4.78	2.58, 2.51			
	^{13}C		54.0	39.7			
Gln-64	^{1}H [^{15}N]	8.57 [123.7]	4.41	2.51, 2.08			H^ϵ = 7.44, 6.94; N^ϵ = 111.9
	^{13}C		54.2	25.9	30.9	177.5	
Ser-65	^{1}H [^{15}N]		4.77	4.01, 3.73			
	^{13}C		56.2	63.6			
*Phe-66	^{1}H [^{15}N]		4.44			7.56	H^ϵ = 7.45; H^ζ = 7.35
	^{13}C		59.4	42.3	137.2	130.3	C^ϵ = 129.2; C^ζ = 128.3
*Leu-67	^{1}H [^{15}N]	10.48 [122.4]	4.33	1.72, 1.36			
	^{13}C		52.9	40.9			
Asp-68	^{1}H [^{15}N]	8.74 [123.8]	4.65	3.12, 2.62			
	^{13}C		50.7	39.8			
Asp-69	^{1}H [^{15}N]	8.40 [118.0]	4.33	2.74, 2.59			
	^{13}C		56.4	38.8	177.2		
Asp-70	^{1}H [^{15}N]	8.23 [122.1]	4.45	2.86, 2.67			
	^{13}C		55.9	38.5			
Gln-71	^{1}H [^{15}N]	8.70 [124.2]	4.29	2.54, 1.74	2.76, 2.19		H^ϵ = 7.37, 6.47
							N^ϵ = 111.8
	^{13}C		57.3	27.3	32.7	177.3	
Ile-72	^{1}H [^{15}N]	8.45 [122.1]	3.99	2.05	1.69, 1.06	0.80, 0.80	$(CH_3)^\gamma$ = 0.99
	^{13}C		62.9	36.0	27.5	10.7	$(CH_3)^\gamma$ = 15.5; C′ = 180.1
Glu-73	^{1}H [^{15}N]	8.48 [125.0]	4.08	2.25, 2.20	2.43, 2.36		
	^{13}C		57.7	27.6	34.7		C′ = 176.2
Ala-74	^{1}H [^{15}N]	7.74 [120.5]	4.31	1.75			
	^{13}C		51.2	17.7			C′ = 175.5
Gly-75	^{1}H [^{15}N]	7.79 [104.6]	(4.33, 3.78)				
	^{13}C		43.3				C′ = 173.0
Tyr-76	^{1}H [^{15}N]	7.96 [120.1]	5.02	2.79, 2.67		7.33	H^ϵ = 6.77
	^{13}C		59.5	37.5	130.7	131.4	C^ϵ = 116.6; C^ζ = 150.2
Val-77	^{1}H [^{15}N]	8.68 [119.1]	4.83	1.57	0.71, 0.60		
	^{13}C		57.3	35.2	20.6, 20.1		
Leu-78							
*Thr-79	^{1}H [^{15}N]		4.43	4.17	1.18		
	^{13}C		60.2	68.3	20.0		
Cys-80							
*Val-81	^{a}H [^{15}N]		4.74				
	^{13}C		52.0	29.6	21.8		
Ala-82	^{1}H [^{15}N]	6.36 [122.6]	5.14	1.07			
	^{13}C		48.6	20.3			C′ = 174.4

Table I (Continued)

residue		H^N [N]	α	β	γ	δ	others
Tyr-83	^1H [^{15}N]	9.13 [125.2]	5.49	3.21, 2.88		7.13	H^ϵ = 6.43
	^{13}C		53.2	38.1	128.4	132.1	C^ϵ = 116.4; C^ζ = 156.0; C′ = 173.9
Pro-84	^1H [^{15}N]	[137.8]	4.73	2.21, 1.99		4.41, 4.09	
	^{13}C		62.0	29.5	26.5	48.9	C′ = 174.9
Thr-85	^1H [^{15}N]	8.46 [111.7]	4.23	4.44	1.11		
	^{13}C		58.6	66.8	21.6		C′ = 170.6
Ser-86	^1H [^{15}N]	7.73 [118.8]	3.57	4.09, 3.74			
	^{13}C		56.1	64.4			C′ = 170.2
Asp-87	^1H [^{15}N]	8.54 [119.3]	5.33	2.76, 2.61			
	^{13}C		55.0	38.4			C′ = 178.2
Val-88	^1H [^{15}N]	9.05 [126.6]	4.92	1.92	1.01, 0.89		
	^{13}C		59.1	35.9	21.4, 21.4		C′ = 172.5
Val-89	^1H [^{15}N]	8.55 [128.5]	4.78	2.03	0.92, 0.87		
	^{13}C		60.3	31.7	18.9, 19.8		C′ = 173.3
Ile-90	^1H [^{15}N]	9.46 [128.8]	4.91	1.51	1.44, 0.82	0.49	$(CH_3)^\gamma$ = 0.71
	^{13}C		57.7	41.7	27.0	12.9	$(CH_3)^\gamma$ = 14.5
Gln-91	^1H [^{15}N]	9.21 [127.3]	5.47	2.30, 2.09	2.30, 2.18		H^ϵ = 7.25, 6.52
							N^ϵ = 110.9
	^{13}C		52.3	27.5	31.8	177.0	C′ = 175.2
Thr-92	^1H [^{15}N]	9.12 [116.7]	4.56	4.67	1.18		
	^{13}C		59.8	67.3	21.1		C′ = 172.6
His-93	^1H [^{15}N]	9.14 [113.8]	4.52	3.39, 3.31		$H\delta^2$ = 7.18	$H^{\epsilon 1}$ = 7.81; $N^{\delta 1}$ = 243.1; $N^{\epsilon 2}$ = 168.6
	^{13}C		57.2	24.6	138.0	$C^{\delta 2}$ = 116.3	$C^{\epsilon 1}$ = 136.5; C′ = 176.7
Lys-94	^1H [^{15}N]	7.43 [115.3]	4.74	1.21	2.36	1.73	H^ϵ = 3.01; N^ζ = 33.5
	^{13}C			31.1	23.1	27.5	C^ϵ = 40.3
Glu-95	^1H [^{15}N]	8.33 [122.9]	3.12	1.94	2.13		
	^{13}C		59.4	27.7	33.9	179.0	C′ = 175.7
Glu-96	^1H [^{15}N]	8.65 [114.7]	3.79	2.09, 2.05	2.32, 2.28		
	^{13}C		56.8	27.5			C′ = 176.0
Asp-97	^1H [^{15}N]	7.87 [120.4]	4.39	2.94			
	^{13}C		53.7	39.7			C′ = 175.8
Leu-98	^1H [^{15}N]	7.81 [119.1]	3.99	1.66, 1.33	1.14	0.60, 0.00	
	^{13}C		53.1	39.6	25.2	24.6, 19.6	
Tyr-99	^1H [^{15}N]	7.07 [125.2]	4.38	3.17, 2.81		7.13	H^ϵ = 6.79
	^{13}C		57.4	38.3	130.7	116.6	C^ϵ = 131.6; C^ζ = 155.5

[a] The ^{13}C and ^{15}N assignments are described in the second paper of this series (Oh et al., 1990). The asterisks (*) indicate amino acid residues whose spin systems are partly observed in two-dimensional NMR spectra due to the paramagnetic perturbation.

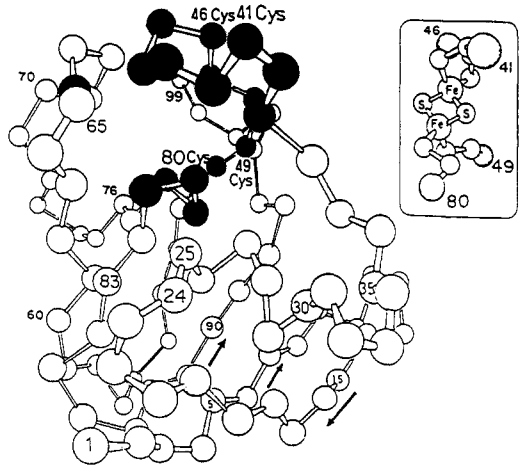

FIGURE 9: Crystal structure of the ferredoxin from *Spirulina platensis* [figure adapted from Figure 4 in Fukuyama et al. (1980)]. For clarity, the iron–sulfur cluster has been removed from the structure and is shown in the inset. The black circles indicate amino acid residues whose $^1H^\alpha$,$^1H^N$ cross peaks were not observed in the fingerprint region of both COSY and NOESY spectra of the related *Anabaena* 7120 ferredoxin.

a loop structure that tightly surrounds the 2Fe·2S* center (Tsukihara, 1981).

Since we have established the similarity of the protein structure in solution (in the diamagnetic part of the protein), it is reasonable to expect that the region around the iron–sulfur cluster also is similar. Given this assumption, it is clear from figure 9 that the experimental absence of all $^1H^\alpha$,$^1H^N$ cross peaks, with the exception of that of Ser^{65} whose absence is attributed to water-peak irradiation effect, can be attributed to paramagnetic perturbation, rather than to some other mechanism such as rapid solvent exchange of amide protons.

The paramagnetism of the 2Fe·2S* cluster of *Anabaena* 7120 ferredoxin can be evaluated by measuring distances between the 2Fe·2S* center and the perturbed amino acids. The amino acids near the 2Fe·2S* center are highly conserved (Tsukihara et al., 1981), probably so as to maintain the protein structure around the iron–sulfur cluster. The distances, as measured on the crystal structure of the related ferredoxin from *Spirulina platensis*, are summarized in Table II, which reports the distances between perturbed backbone protons and two iron atoms. Accurate definition of the paramagnetic region is complicated by the presence of two iron atoms and by the dihedral angle dependence of cross-peak intensities in COSY and NOESY spectra. The paramagnetic line broadening effect falls off as $1/d^6$, where d is the separation between the paramagnetic center and the resonating nucleus (Phillips & Poe, 1973). Assuming that the paramagnetic character of both of the iron atoms is the same, we introduce a reduced distance, d_r, which is defined as $[2d_1^6d_2^6/(d_1^6 + d_2^6)]^{1/6}$. In this treatment, a nucleus at distances d_1 and d_2 from Fe^1 and Fe^2 would be affected the same as a hypothetical nucleus equidistant (d_r) from both iron atoms. From Table II, d_r of 7.87 Å (H^α of Phe^{66}) is the farthest distance we did not observe COSY or NOE cross peaks from its own or adjacent amino acids. A computer-aided search revealed that no assigned amino acids showed d_r shorter than 7.87 Å except Leu^{67} $^1H^N$, whose d_r is 7.83 Å. The $^1H^\alpha$,$^1H^N$ cross peak of Leu^{67} was only weakly observed in the COSY (Figure 1) and NOESY spectrum. The H^N of this residue exchanged slowly with solvent, and its signal is resolved from other amide proton

Table II: Distances (Å) between the Two Iron Atoms of the 2Fe·2S* Center and the H^{α} and H^N of Amino Acids Whose Resonances Were Not Observed in the Fingerprint Region of COSY and NOESY Spectra[a]

residue		distance Fe1, d_1	distance Fe2, d_2	d_r	residue		distance Fe1, d_1	distance Fe2, d_2	d_r
Phe^{39}[b]	H^{α}	4.49	4.41	4.45	Thr^{48}	H^{α}	6.93	6.91	6.92
	H^N	6.90	7.20	7.04		H^N	5.10	5.70	5.34
Ser^{40}	H^{α}	5.18	7.00	5.67	Cys^{49}	H^{α}	6.26	4.88	5.30
	H^N	3.30	4.38	3.60		H^N	5.83	4.84	5.18
Cys^{41}	H^{α}	4.76	6.94	5.26	Ala^{50}	H^{α}	8.23	6.05	6.63
	H_N	4.48	6.29	4.92		H^N	7.41	5.94	6.41
Arg^{42}	H^{α}	3.10	3.23	3.16	Ser^{65}[c]	H^{α}	13.75	12.20	12.82
	H^N	2.43	3.87	2.70		H^N	13.97	12.04	12.76
Ala^{43}	H^{α}	6.38	6.08	6.22	Phe^{66}	H^{α}	9.07	7.30	7.87
	H^N	3.79	4.36	4.00		H^N	11.70	9.76	10.43
Gly^{44}	H^{α}	4.57	4.03	4.24	Leu^{78}	H^{α}	10.74	5.66	6.33
	H^{α}	6.30	5.54	5.84		H^N	8.09	8.33	8.20
	H^N	5.46	4.68	4.97	Thr^{79}	H^{α}	10.39	7.86	8.57
Ala^{45}	H^{α}	6.85	7.60	7.16		H^N	8.82	6.35	6.97
	H^N	4.27	5.15	4.57	Cys^{80}	H^{α}	7.20	5.17	5.68
Cys^{46}	H^{α}	5.12	6.44	5.54		H^N	7.01	4.51	5.00
	H^N	3.63	4.64	3.94	Val^{81}	H^{α}	10.23	8.32	8.95
Ser^{47}	H^{α}	5.98	5.50	5.71		H^N	8.47	6.20	6.79
	H^N	5.15	5.99	5.46					

[a] The proton-added 2.5-Å X-ray coordinates of *Spirulina platensis* ferredoxin were used. Distances were calculated from the coordinates of *S. platensis* ferredoxin (Tsukihara et al., 1981). Distance d_1 is to the iron atom (Fe1) ligated to Cys^{41} and Cys^{46}; distance d_2 is to the iron atom (Fe2) ligated to Cy^{49} and Cys^{80}; distance d_r is the reduced distance (see text). [b] Residue 39 in *S. platensis* ferredoxin is tyrosine, which is replaced by phenylalanine in *Anabaena* 7120 ferredoxin. The distances of the H^{α} and H^N from the iron atoms are assumed to be identical in both proteins. [c] The absence of the Ser^{65} $^1H^{\alpha}$,$^1H^N$ cross peak in the fingerprint region of the COSY spectrum is attributed to water-peak irradiation.

resonances (Figure 1), which allowed determination of the T_1 of the resonance. The measured T_1 of Leu^{67} $^1H^N$ (58 ms) was about 7 times shorter than any other diamagnetic amide resonances. In addition to paramagnetic line broadening, the $^1H^{\alpha}$,$^1H^N$ cross peak from Phe^{66} may be diminished by the small coupling constant, $^3J_{\alpha N}$. Thus, roughly speaking, cross peaks in homonuclear ^1H 2D NMR spectra are not observed from protons that are closer than d_r = 7.8 Å to both iron atoms.

Since broad, paramagnetically shifted peaks from the protons closest to the irons are readily observed in 1D ^1H NMR spectra (Oh & Markley, 1990), we speculate that the unobserved ^1H resonances reside within the diamagnetic envelope of the NMR spectrum but have line widths too broad to produce observable cross peaks in homonuclear ^1H 2D NMR spectra.

Prospects. The hyperfine-shifted ^1H, ^{13}C, and ^{15}N peaks of *Anabaena* 7120 show drastic differences in the two oxidation states (data not shown). However, the ^1H COSY NMR spectrum of the reduced *Anabaena* ferredoxin (data not shown) is similar to that of the oxidized protein. These comparisons indicate that a considerable change in the paramagnetic character of the 2Fe·2S* center occurs upon reduction but that it is not accompanied by a gross conformational change of the protein. We expect that assignments of the diamagnetic resonances of reduced ferredoxin (work in progress) will provide a useful comparison of the paramagnetic character of the reduced and oxidized 2Fe·2S* center. Finally, it will be of great interest to define the spatial topology of paramagnetism of other iron–sulfur cluster types by this approach.

Acknowledgments

We thank Dr. E. S. Mooberry for assistance with NMR instrumentation and B. J. Stockman for help in preparing the protein samples.

References

Aketagawa, J., & Tamura, G. (1980) *Agric. Biol. Chem. 44*, 2371–2378.

Alam, J., Whitaker, R. A., Krogman, D. W., & Curtis, S. E. (1986) *J. Bacteriol. 168*, 1265–1271.

Anderson, A. J., Dunham, W. R., Sands, R. H., Bearden, A. J., & Crespi, H. L. (1975) *Biochim. Biophys. Acta 408*, 306–318.

Bodenhausen, G., Kogler, H., & Ernst, R. R. (1984) *J. Magn. Reson. 58*, 370–388.

Cammack, R., Roa, K. K., Bargeron, C. P., Hutson, K. G., Andrew, P. W., & Rogers, L. J. (1977) *Biochem. J. 168*, 205–209.

Chan, T.-M., & Markley, J. L. (1983a) *Biochemistry 22*, 5982–5987.

Chan, T.-M., & Markley, J. L. (1983b) *Biochemistry 22*, 5996–6002.

Chan, T.-M., Hermodson, M. A., Ulrich, E. L., & Markley, J. L. (1983) *Biochemistry 22*, 5988–5995.

Davis, D. G., & Bax, A. (1985) *J. Am. Chem. Soc. 107*, 2820–2821.

Englander, S. W., & Wand, A. J. (1987) *Biochemistry 26*, 5953–5958.

Fukuyama, K., Hase, T., Matsumoto, S., Tsukihara, T., Katsube, Y., Tanaka, N., Kakudo, M., Wada, K., & Matsubara, H. (1980) *Nature 286*, 522–524.

Hase, T., Wakabayaski, S., Matsubara, H., Rao, K. K., Hall, D. O., Widmer, H., Gysi, J., & Zuber, H. (1978) *Phytochemistry 17*, 1863–1867.

Ho, K. K., Ulrich, E. L., Krogmann, D. W., & Gomez-Lojero, C. (1979) *Biochim. Biophys. Acta 545*, 236–248.

Hoult, D. I., & Richards, R. E. (1975) *Proc. R. Soc. London A34*, 311–340.

Ida, S. (1977) *J. Biochem. 82*, 915–918.

Lea, P. J., & Miflin, B. J. (1974) *Nature 251*, 614–616.

Macura, S., & Wüthrich, K. (1982) *J. Magn. Reson. 46*, 269–282.

Marion, D., & Wüthrich, K. (1983) *Biochem. Biophys. Res. Commun. 113*, 967–974.

Masaki, R., Yoshikawa, S., & Matsubara, H. (1982) *Biochim. Biophys. Acta 700*, 101–109.

Mooberry, E. S., Oh, B.-H., & Markley, J. L. (1989) *J. Magn. Reson. 85*, 147–149.

Oh, B.-H., & Markley, J. L. (1989) *Biopolymers 28*, 1833-1837.
Oh, B.-H., & Markley, J. L. (1990) *Biochemistry* (third paper of three in this issue).
Oh, B.-H., Westler, M. W., Darba, P., & Markley, J. L. (1988) *Science 240*, 908-911.
Oh, B.-H., Westler, W. M., Markley, J. L. (1989) *J. Am. Chem. Soc. 111*, 3083-3085.
Oh, B.-H., Mooberry, E. S., & Markley, J. L. (1990) *Biochemistry* (second paper of three in this issue).
Phillips, W. D., & Poe, M. (1973) in *Iron Sulfur Proteins* (Lovenberg, W., Ed.) Vol. II, pp 255-284, Academic Press, New York and London.
Poe, M., Phillips, W. D., Glickson, J. D., McDonald, C. C., & San Pietro, A. (1971) *Proc. Natl. Acad. Sci. U.S.A. 68*, 68-71.
Rance, M., Sørensen, O. W., Bodenhausen, G., Wagner, G., Ernst, R. R., & Wüthrich, K. (1983) *Biochem. Biophys. Res. Commun. 117*, 479-485.
Salmeen, I., & Palmer, G. (1972) *Arch. Biochem. Biophys. 150*, 767-773.
Shaka, A. J., Keeler, J., Frenkiel, T., & Freeman, R. (1983) *J. Magn. Reson. 52*, 335-338.
Shon, K., & Opella, S. J. (1989) *J. Magn. Reson. 82*, 193-197.
Stockman, B. J., Westler, W. M., Darba, P., & Markley, J. L. (1988a) *J. Am. Chem. Soc. 110*, 4095-4096.
Stockman, B. J., Westler, W. M., Mooberry, E. S., & Markley, J. L. (1988b) *Biochemistry 27*, 136-142.
Stockman, B. J., Reily, M. D., Westler, W. M., Ulrich, E. L., & Markley, J. L. (1989) *Biochemistry 28*, 230-236.
Trebst, A., & Avron, M., Eds. (1977) *Photosynthesis*, Vol. I, Photosynthetic Electron Transport and Photophosphorylation, Springer-Verlag, New York.
Tsukihara, T., Fukuyama, K., Nakamura, M., Katsube, Y., Tanaka, N., Kakudo, M., Wada, K., Hase, T., & Matsubara, H. (1981) *J. Biochem. 90*, 1763-1773.
Tsukihara, T., Fukuyama, K., & Katsube, Y. (1986) in *Iron-Sulfur Protein Research* (Matsubara, H., et al., Eds.) pp 59-68, Japan Science Society Press, Tokyo.
Tsutusi, T., Tsukihara, T., Fukuyama, K., Katsube, Y., Hase, T., Matsubara, H., Nishikawa, Y., & Tanaka, N. (1983) *J. Biochem. 94*, 299-302.
Westler, W. M., Kainosho, M., Nagao, H., Tomonaga, N., & Markley, J. L. (1988) *J. Am. Chem. Soc. 110*, 4093-4095.
Wüthrich, K. (1986) *NMR of Proteins and Nucleic Acids*, pp 130-161, Wiley, New York.

Multinuclear Magnetic Resonance Studies of the 2Fe·2S* Ferredoxin from *Anabaena* Species Strain PCC 7120. 2. Sequence-Specific Carbon-13 and Nitrogen-15 Resonance Assignments of the Oxidized Form†

Byung-Ha Oh, Eddie S. Mooberry, and John L. Markley*

Department of Biochemistry, College of Agricultural and Life Sciences, University of Wisconsin—Madison, 420 Henry Mall, Madison, Wisconsin 53706

Received October 19, 1989

ABSTRACT: Multinuclear two-dimensional NMR techniques were used to assign nearly all diamagnetic ^{13}C and ^{15}N resonances of the plant-type 2Fe·2S* ferredoxin from *Anabaena* sp. strain PCC 7120. Since a ^{13}C spin system directed strategy had been used to identify the ^{1}H spin systems [Oh, B.-H., Westler, W. M., & Markley, J. L. (1989) *J. Am. Chem. Soc. 111*, 3083-3085], the sequence-specific ^{1}H assignments [Oh, B.-H., & Markley, J. L. (1990) *Biochemistry* (first paper of three in this issue)] also provided sequence-specific ^{13}C assignments. Several resonances from ^{1}H–^{13}C groups were assigned independently of the ^{1}H assignments by considering the distances between these nuclei and the paramagnetic 2Fe·2S* center. A ^{13}C–^{15}N correlation data set was used to assign additional carbonyl carbons and to analyze overlapping regions of the ^{13}C–^{13}C correlation spectrum. Sequence-specific assignments of backbone and side-chain nitrogens were based on ^{1}H–^{15}N and ^{13}C–^{15}N correlations obtained from various two-dimensional NMR experiments.

Until recently, extensive assignments in NMR[1] spectra of proteins have been confined to protons, and the wealth of information provided by ^{13}C and ^{15}N nuclei was largely neglected. Although sequence-specific ^{1}H resonance assignments are available for about 60 small proteins [for a review, see Markley (1989)], extensive ^{13}C assignments are limited to only three proteins: bovine pancreatic trypsin inhibitor (Wagner & Brühwiler, 1986), turkey ovomucoid third domain (Robertson et al., 1989), and staphylococcal nuclease (Wang et al., 1990). Extensive backbone nitrogen assignments are limited to bovine pancreatic trypsin inhibitor (Glushka & Cowburn, 1987), staphylococcal nuclease (Torchia et al., 1989; Wang et al., 1990), inflammatory protein C5a (Zuiderweg & Fesik, 1989), DNA binding protein Ner from phage Mu (Gronen-

† This work was supported by USDA Competitive Grant 88-37262-3406 and National Institutes of Health Grant RR02301 from the Biomedical Research Technology Program, Division of Research Resources, and made use of the National Magnetic Resonance Facility at Madison, which is supported in part by Grant RR023021. Additional equipment in the facility was purchased with funds from the University of Wisconsin, the NSF Biological Biomedical Research Technology Program (Grant DMB-8415048), the NIH Shared Instrumentation Program (Grant RR02781), and the U.S. Department of Agriculture. B.-H.O. is supported by a Peterson Fellowship from the University of Wisconsin—Madison.

* To whom correspondence should be addressed.

[1] Abbreviations used are defined in Oh and Markley (1990a).

0006-2960/90/0429-4004$02.50/0